The exoskeleton technology as a solution to seismic adjustment of existing buildings

Available online at www.sciencedirect.com

ScienceDirect

Procedia Structural Integrity 26 (2020) 175–186

Structural Integrity Procedia

www.elsevier.com/locate/procedia

The 1st Mediterranean Conference on Fracture and Structural Integrity, MedFract1

# The exoskeleton technology as a solution to seismic adjustment of existing buildings

L. Martelli[a]*, L. Restuccia[a], G.A. Ferro[a]

[a] *Department of Structural, Geotechnical and Building Engineering (DISEG), Politecnico di Torino, Turin, Italy*

**Abstract**

The high seismic vulnerability of the Italian territory and its ancient building heritage require attention regarding planning interventions on existing buildings. In fact, they show both structural and technological design deficiencies mainly due to the period of construction, the lack of design to withstand horizontal forces and the type of material used, which is mainly masonry and reinforced concrete. Therefore, it is extremely difficult to intervene with solutions of seismic improvement or adjustment also concerning the economic point of view. This work suggests an advanced approach to address the problem employing the innovative concept of an external self-supporting steel system: the exoskeleton technology. It has been applied to guarantee the seismic adjustment of an existing structure that aims at reaching higher safety targets as well as new aesthetic and sustainable features. Due to the overcoming of lifespan limit of 50 years, the explored residential construction no longer complies with the current technical standards; the issue has been solved connecting the two structures by a non-dissipative rigid link to create a coupled system whose floors show an in-plane rigid behaviour while maintaining separated their response to seismic actions. Initial explanations of the internal and the outer constructions advance the dynamic analysis, which allows to highlight the main seismic properties of the whole model such as frequencies and periods of vibration, floor displacements and shear forces. Following outcomes do not just focus on how the exoskeleton can take base and floor shear forces but also the way it manages to strongly reduce displacements and deformations of the primary building, so that it can bear earthquake actions preventing not only collapse but also reducing non-structural elements damage.



*Keywords:* Coupled system; exoskeleton structure; retrofitting; seismic adjustment; structural dynamics

* Corresponding author. Tel.: +39 011 090 4849.
*E-mail address:* lucrezia.martelli@polito.it


10.1016/j.prostr.2020.06.021

## 1. Introduction

Structures have a significant role for populations everywhere in the world; on the other hand, they cause considerable effects to the environment from initial construction works to the energy consumption during its lifespan, no matter what they have been designed for. As reported in the Document for E2B European Initiative (2012), more than a third of total greenhouse gas emissions originates from them; at the same time, this energy-intensive field represents the "second largest untapped cost-effective potential for energy savings after the energy sector". Thus, innovative ideas and advanced technological solutions should guide the experts to take safer and more sustainable measures that must be applied above all to existing buildings, as already suggested by Martelli L. et al. (2019).

The priceless Italian building heritage, whose variety of styles makes it unique, unfortunately hides a critical aspect: it is generally outdated. In fact, it has been proved that almost 61% of total constructions has already exceeded the designed lifespan of 50 years; in addition, more than a half of them was built without considering seismic design principles nor energy consumption as illustrated by ISTAT census (2011). The noteworthy result shows an evident lack of adequate seismic designs related to the original documentation and recent energetic monitoring as well; so, safety assessment and structural vulnerability should finally take a primary role to counteract the growing degradation. Hence, the present study aims at exploring the seismic performance of a steel exoskeleton structure applied to a residential complex and the way this solution succeeds in controlling earthquake induced vibrations of that existing reinforced concrete building.

The term exoskeleton structure indicates a self-supporting structural system placed in the exterior part of an existing construction which is connected to. The chosen connection also represents the way the internal building can unload itself giving the stresses to the steel external frame, which is essentially designed to protect the first one as described by Belleri et al. (2016), Caverzan A. (2016) and Marini A. (2014). Researchers have become more and more interested in this type of method trying to assure not only retrofitting renovations like those related to energy efficiency, architectural renewal or environmental sustainability, but especially in engineering approaches: it is necessary that anti-seismic strategies join the previous subjects, as reported by Reggio et al. (2019). As highlighted in Martelli L. et al. (2019), external structures allow to reduce business downtime and to avoid residents' relocation thanks to the operative processes that are completed from the outside; they can also enhance economic and environmental effectiveness of the resulting system by updating the existing construction to the current sustainable needs; moreover, they restore the designed lifetime bringing also a new aesthetic shape and additional housing or public spaces can be provided as well. The exoskeleton is added to bear seismic loads aiming at protecting the existing frame structure and preventing its damage during earthquake actions. A rigid link is assumed to connect the two independent structures whose masses are not negligible so, as outlined by Reggio et al. (2019), a dynamic coupling has been considered.

The paper is organized as follows: After this Introduction, Section 2 focuses on a theoretical description of the resulting system composed by two coupled linear viscoelastic oscillators according to their dynamic model. A more detailed case study is carried on in Section 3: firstly, the existing inner building, then its seismic adjustment. Subsections 3.3 and 3.4 concern dynamic results of both structural models comparing each other; in Section 4, conclusions are finally explained.

## 2. Theoretical model

A dynamic analysis is conducted by the discretization of the existing building into a planar frame that consists of rigid stories whose masses are centred on each horizontal level; stiffness, instead, is referred to the columns that connect one floor to the other. A theoretical simplification consists of getting the system equivalent to a simple oscillator with one degree of freedom, i.e. mass is concentrated in a single point, a spring without mass holds all the stiffness and a damper makes energetic dissipation possible, as detailed by Martelli L. (Master Degree Thesis, 2018). So, without lack of generality, the resulting system composed by a primary building linked to an exoskeleton structure is modelled by means of two coupled linear viscoelastic oscillators, as reported by Reggio et al. (2019). In fact, the first oscillator represents the existing construction denoted by 1 as a subscript; on the contrary, the secondary one indicates the external structure that uses 2 as a subscript. In both cases, $M_i$ $K_i$ and $C_i$ indicate mass stiffness and dumpling coefficients of the i-th oscillator, while $X_i(t)$ is its displacement; the connection is considered to be non-dissipative with a Hooke spring, whose stiffness is represented by coefficient $K$ (Figure 1). Denoting relative displacements with $U_i$, the dynamic equilibrium derived from ground motion $X_g(t)$ is:

$$M_1\ddot{U}_1 + C_1\dot{U}_1 + K_1U_1 = -M_1\ddot{X}_g + K(U_2 - U_1) \quad (1)$$

with $U_1 = X_1 - X_g$, $U_2 = X_2 - X_g$ and $(\dot{\ })$ symbolising the derivative with respect to time $t$.
According to the suggested connection, the rigid coupling between the two oscillators represents the limit case of the Hooke spring in which stiffness coefficient tends to infinity ($K \rightarrow \infty$). Therefore, $U_2 \rightarrow U_1$ and it is possible to verify the previous assumption of a Single-Degree-Of-Freedom (SDOF) system modifying Eq. (1) into the following one:

$$(M_1 + M_2)\ddot{U}_1 + (C_1 + C_2)\dot{U}_1 + (K_1 + K_2)U_1 = -(M_1 + M_2)\ddot{X}_g \quad (2)$$

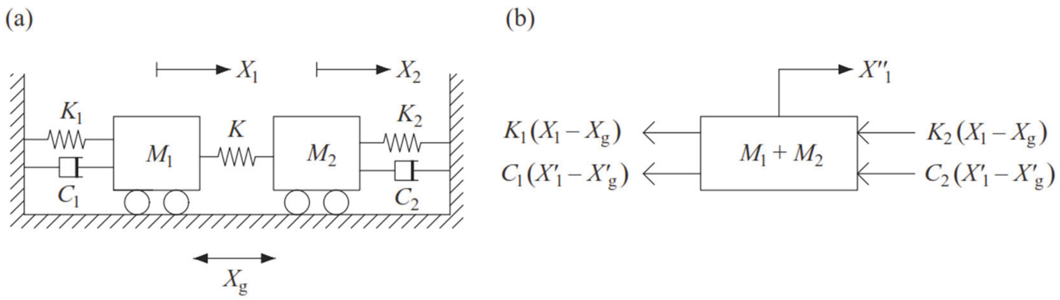


Fig. 1. Coupled system: (a) structural model; (b) free body diagram for a rigid coupling (K→∞).

## 3. Case study

On the back of the survey explored by Reggio et al. (2019), this chapter deals with the seismic response of an existing building (a multi-degree-of-freedom frame structure) which represents a real case study in order to examine how it behaves when a rigid link connects the former to an exoskeleton structure.
A linear dynamic (also called modal) analysis has been pursued to obtain elastic pseudo-acceleration response spectra, peak floor displacements, inter-storey drift ratios and the amount of base shears acting on the system; then, the regularity of the new structure and the price for the steel adjustment have been checked to better understand the effectiveness of the model.

### *3.1 Existing structure*

The primary structure is a flat complex situated in the south west area of Turin, in Italy. It is an isolated reinforced concrete building made up of nine stories over the basement: inter-storey heights are generally equal to 3.27 m, except for the lowest pilotis level that reaches 5.07 m; floor plans are characterized by a quite regular shape whose dimension along x-axis is approximately twice as it is along the transverse one, as clearly deductible from the values of nearly 27.50 m x 16.20 m (Fig. 2):

This building dates to the end of the ’50s since construction works started in 1957 and finished two years later, which highlights the critical issue of exceeding the designed lifespan as specified by the new technical regulations. It is a monodirectional reinforced concrete frame with vertical structural elements arranged in regular interaxle spacings. The detailed documentation has provided both columns and beams sections as well as their reinforcements, then it has allowed to discover that reinforced concrete slabs have a thickness of 16+4 cm. Concrete that has been used was a C16/20-type, so its characteristic compressive strength is equal to $f_{ck} = 16\ MPa$; talking about the structural steel employed, it is a no more commercial kind with low properties.

The last characterization concerns the subsoil, which belongs to type C, i.e. “Sediments of coarse-grained moderately thickened soils or fine-grained moderately compact soils”, as defined in the Italian Building Code NTC (2018).

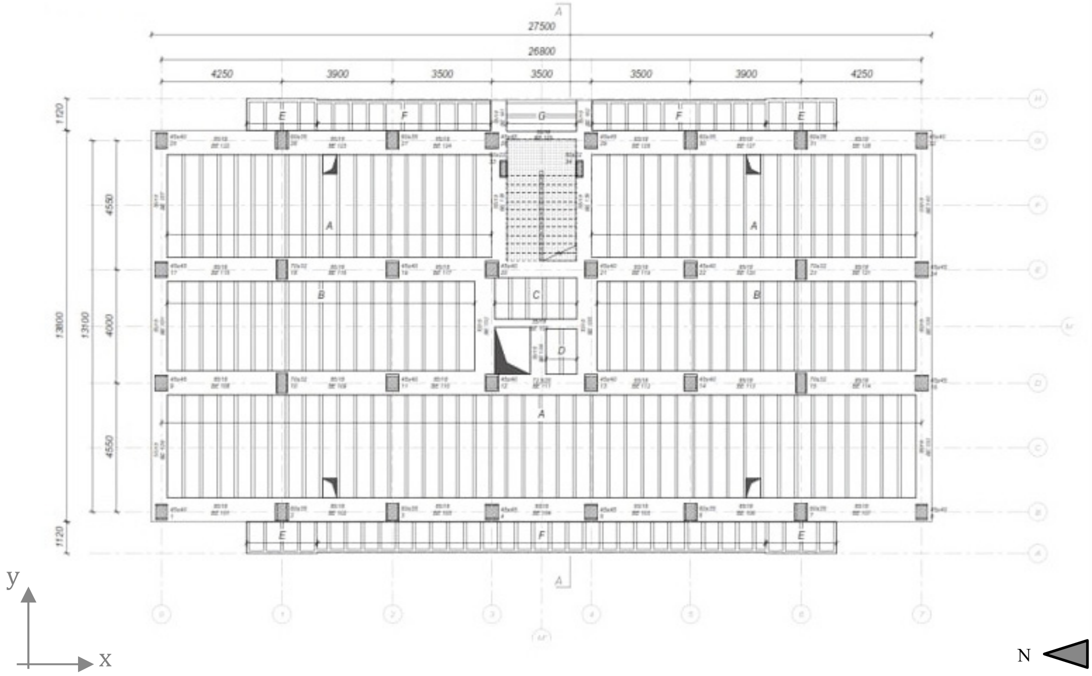


Fig. 2. Structural plan of a standard floor.

Subsequently, a Finite Element (FE) model has been created using the structural analysis software Robot Structural Analysis Professional Autodesk (2020).

For the sake of simplicity, from now on the capital letter *U* stands for "Uncontrolled structure" to distinguish it from *C* referred to the final "Coupled system".

### *3.1.1 FE model*

A reinforced concrete moment-resisting frame has been designed with uniform planar distribution of mass and stiffness and a non-ductile behaviour. Floor slabs have an in-plane rigid performance, that has been validated thanks to slab thickness equal to 4 cm; indeed, Italian Building Code NTC (2018) explains that "as long as the available openings do not significantly reduce stiffness, horizontal stories may be considered infinitely rigid in their floor plan providing that they have been executed in reinforced concrete or in concrete masonry with at least a 40 mm-thick reinforced concrete slab […]".

Two perspective drawings of the initial model are shown in the following figure:Thus, each level has three degrees of freedom: two translations along x- and y-direction of the centre of gravity for each rigid floor and a rotation about z-axis. For better accuracy, modelling does not concern non-structural elements like partition walls loads, staircases and so on. Following figure (Fig. 4) illustrates a structural axonometric view of the primary construction.

### *3.2 Exoskeleton structure*

A self-supporting steel exoskeleton has been placed next to the existing construction and it rises until the top lying on its own rigid foundations, that have been arranged by the introduction of fixed supports.

It emerges from the basement to the highest floor on the entire façade and its upper elements end over the 9th level; each structural element is a S355-type, no matter if it refers to beams, diagonals or columns. Every node of the exoskeleton has been located outside of the existing floors in order to let the two structures work separately towards the same purpose, that is the improvement in the response of the entire system when subjected to seismic actions. Additionally, in the interests of safety, analyses have been executed setting up a minimum vulnerability index equal to $\zeta_E = 100\%$, as to assure the highest level of adjustment the Italian Standard for Constructions, NTC (2018) grants.

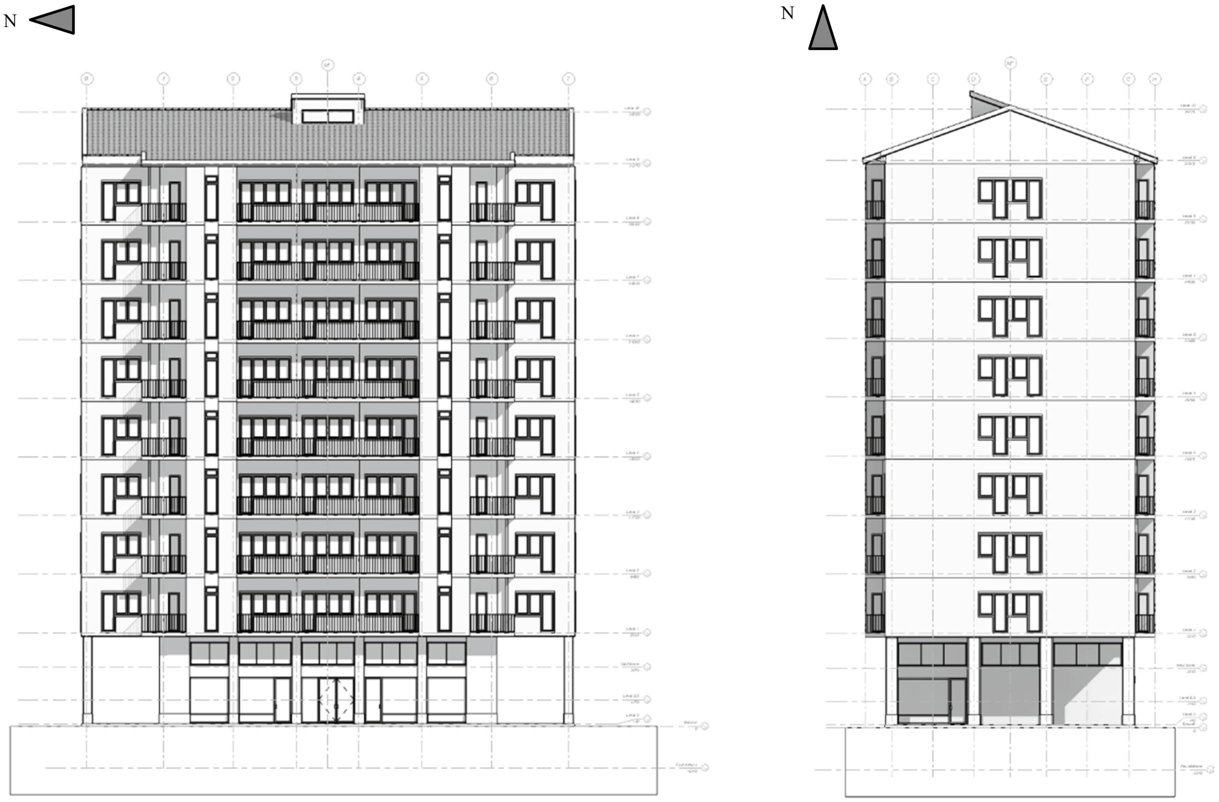


Fig. 3. Perspective views of the original model (U).

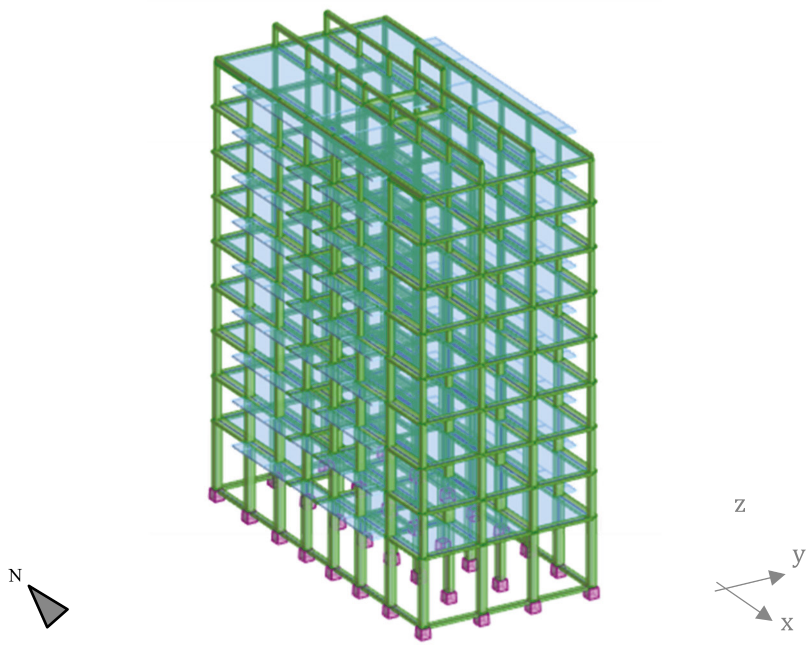


Fig. 4. FE model of the existing structure (U).

The final axonometric model of the retrofitted system appears on the left side of Figure 5, then two perspective drawings are introduced on the right part of the same image. The solution consists of diagonal elements that create a diamond-shaped pattern along x-direction to which vertical and horizontal steel sections are added to stiffen the entire structure; the same goal is reached on the two shorter sides, i.e. those that act along y-direction, thanks to K bracings that are introduced together with steel columns and beams.

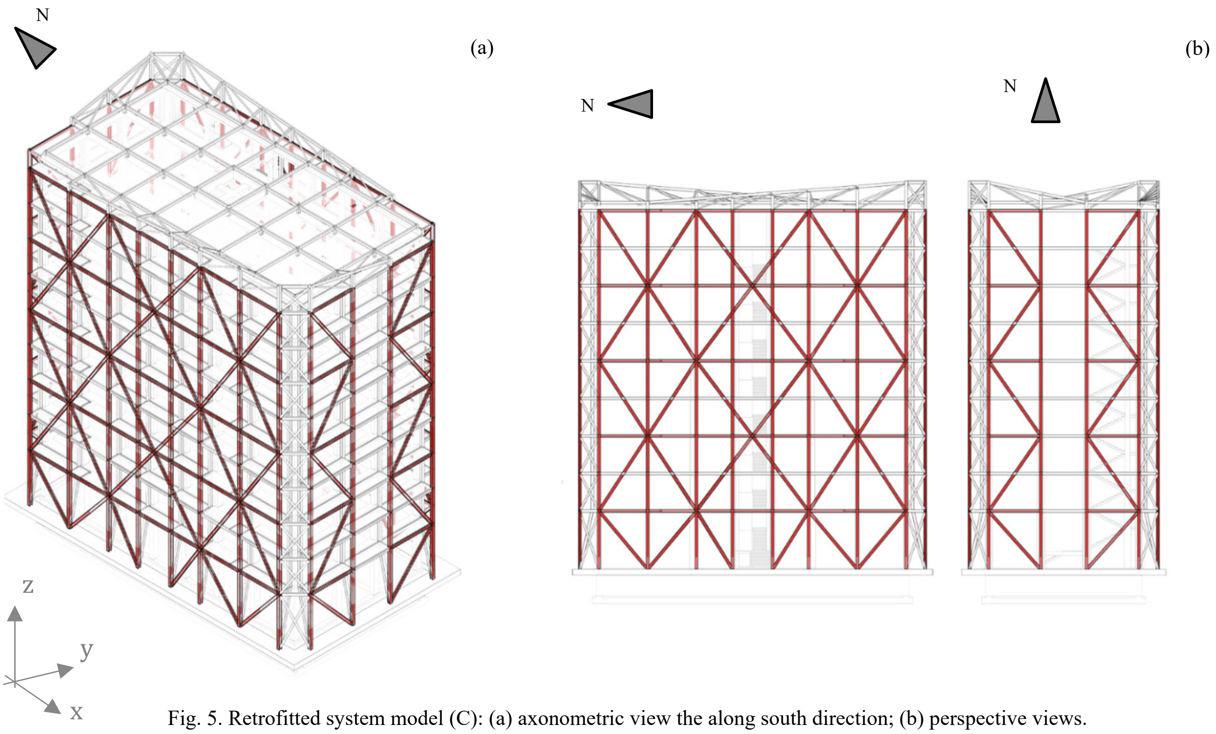

Fig. 5. Retrofitted system model (C): (a) axonometric view the along south direction; (b) perspective views.

Even if the original building was enough regular in plan, the exoskeleton addition has improved its planar regularity, as it can be seen in the next figure (Fig. 6). In fact, there are no distance limitations that should be checked from the

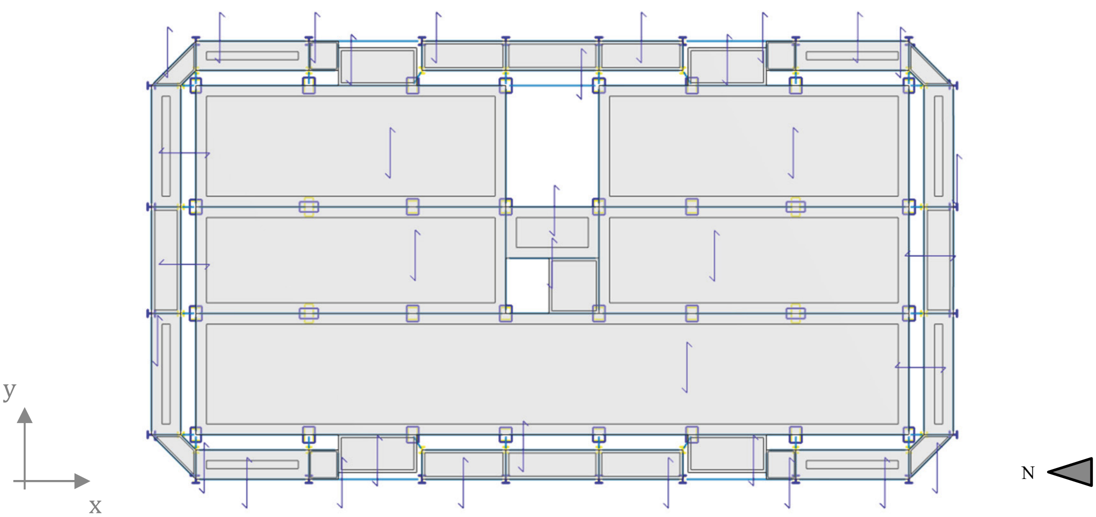

Fig. 6. First floor of the retrofitted system (C).

Interdepartmental Ordinance no.1444 (1968) in case of adjacent buildings, so a rectangular perimeter characterized by diagonal angles has been created aiming at reaching the best alignment with the existing balconies; directions of the slabs can be noticed as well

### *3.3 Modal properties and response spectra*

The table introduced as follows, Table 1, illustrates the comparison between modal properties of the primary construction and those of the controlled system. Thanks to a good planar regularity, there are practically no more rotational modes or their participating mass ratios remain limited when the exoskeleton is introduced:

Table 1. Modal properties of the primary structure and the coupled system: circular frequencies Ω, periods T, participating mass ratios $M_x$ and $M_y$ in x- and y-direction respectively.

| | Primary structure | | | | Coupled system | | | |
|---|---|---|---|---|---|---|---|---|
| Mode | Ω [rad/s] | T [s] | $M_x$ [%] | $M_y$ [%] | Ω [rad/s] | T [s] | $M_x$ [%] | $M_y$ [%] |
| 1 | 3.519 | 1.790 | 0.01 | 78.84 | 4.210 | 1.490 | 0.00 | 81.28 |
| 2 | 3.644 | 1.730 | 52.54 | 0.01 | 6.472 | 0.970 | 84.02 | 0.00 |
| 3 | 3.644 | 1.720 | 27.50 | 0.00 | 8.545 | 0.740 | 0.01 | 0.00 |
| 4 | 9.739 | 0.640 | 0.00 | 11.69 | 16.022 | 0.390 | 0.00 | 11.78 |
| 5 | 10.116 | 0.620 | 8.35 | 0.00 | 20.420 | 0.310 | 10.08 | 0.00 |
| 6 | 10.116 | 0.620 | 3.45 | 0.00 | 27.646 | 0.230 | 0.00 | 0.00 |
| 7 | 16.713 | 0.380 | 0.00 | 3.91 | 28.714 | 0.220 | 0.00 | 3.54 |
| 8 | 16.965 | 0.370 | 3.65 | 0.00 | 32.673 | 0.190 | 3.04 | 0.00 |
| 9 | 17.279 | 0.360 | 0.03 | 0.00 | 38.642 | 0.160 | 0.00 | 1.02 |
| 10 | 23.122 | 0.270 | 0.00 | 1.98 | 42.914 | 0.150 | 1.11 | 0.00 |

The coupled system reveals higher frequencies than those referred to the existing building, because of an increase in stiffness due to the external exoskeleton, as it is described below. Just focusing on the main three modes, the first one goes through a rise of 20% in frequency and the third one becomes more than twice. The values of period rapidly reduce from the original building to the retrofitted system because of a structural stiffening. Moreover, thanks to a greater regularisation given by the exoskeleton, the 2$^{nd}$ mode of vibration becomes entirely translational giving to the third one a mild torsional effect.

Seismic analyses of the two FE models (the primary structure and the coupled system) have been run aiming at identifying their behaviour caused by the action of earthquake forces. The input data are described by pseudo-acceleration response spectra of the examined site that agree with the Italian Building Code, NTC (2018), and particular interest was drawn on Damage and Life-safety Limit States (DLS and LLS respectively); the first one is described by a peak ground acceleration $a_g = 0.029g$ with 63% of exceedance probability during 50 years, while LLS refers to a probability of exceedance equal to 10% in 50 years and it is characterized by a peak ground acceleration equal to $a_g = 0.055g$. These values have been acquired from the Institutional technical agency CSLP (2019) in accordance with national technical regulations NTC (2018).

The above curves have then been deployed to place the points referred to the 10 modes of vibration (taken by the modal analysis performed with Robot Autodesk) for each structural system, so that it could be possible to visualize their coordinates in terms of period and pseudo-acceleration. In the diagrams below the outcomes are displayed (Fig. 7). As it can be seen, the controlled system is characterized by lower periods that correspond to higher pseudo-accelerations, in fact the reference points move to the left and the majority part of them have even reached the plateau: it is the evidence of a greater stiffness due to the addition of the external steel exoskeleton. This behaviour is not related to a specific limit state because it happens for both; corresponding values are lower in case of Damage LS than it is for Life-safety LS, of course.

As a way to compare the results, a supplementary diagram indicates the first three modes of both structures for Life-Safety LS: even if it may not appear so marked, the coupled system reveals a clear increase in acceleration as a proof of stiffness growth due to the steel structure (Fig. 8). This attitude is demonstrated by the rates that have been introduced in Table 2.

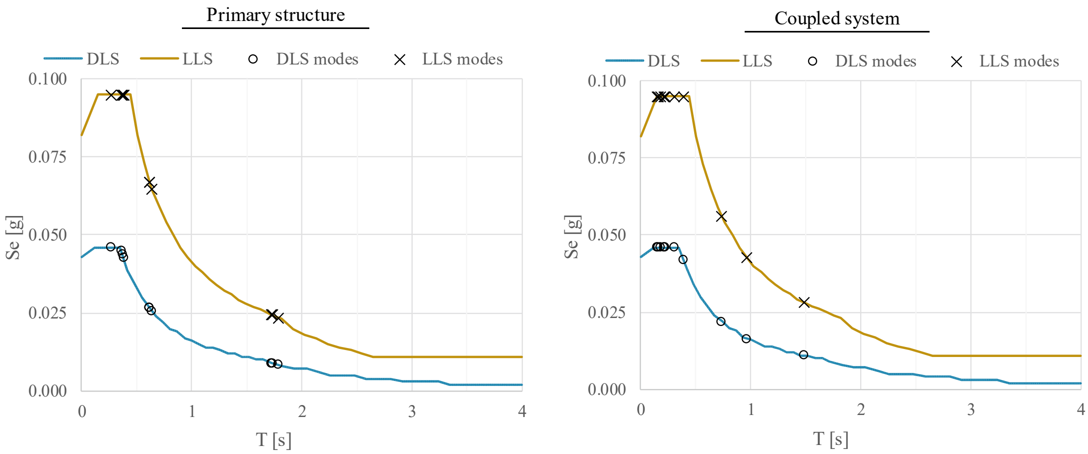


Fig. 7. Horizontal component of elastic pseudo-acceleration response spectra of both structural systems.

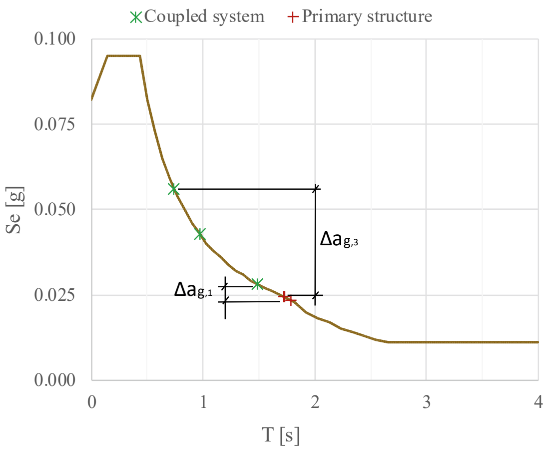


Fig. 8. Elastic pseudo-acceleration response spectrum for the top three vibration modes, LLS.

Table 2. $\Delta a_g$ variations between the two systems.

| Mode | $\Delta a_{g,i}$ variation |
|---|---|
| 1 | 19% |
| 2 | 76% |
| 3 | 129% |

### *3.4 Seismic response*

The linear dynamic analysis has allowed to find seismic response characteristics like maximum floor displacements, inter-storey drift ratios and base shears; they are the main practical quantities to monitor the behaviour of structures from a seismic and vulnerability point of view.

Tables 3 and 4 represent peak floor displacements for which Damage and Life-safety Limit States have been considered for the original structure and the combined primary-exoskeleton system; the former also indicates DLS inter-storey drift ratios.

It may be noted that displacements decrease especially along x-direction reaching the maximum positive result at the top, where Ux reduces by 46%.

Section 7.3.6.1/part (a) of the Italian Building Code, NTC (2018), demands a stiffness verification of CU II-type buildings for Damage Limit State in which inter-storey drift ratios must show data that remain less than or equal to $0.005\ h_i$, where $h_i$ stands for every floor height which is $i = 1 \div 9$ in this case. The existing construction has a constant inter-storey elevation of $3.27\ m$ except for the lowest level which reaches $5.07\ m$; so, maximum value $d_{max} = 0.005\ h_i = 0.02\ m$ refers to the upper floors, while the bottom level corresponds to $d_{max} = 0.005\ h_{1-0} = 0.03\ m$. Consequently, Figure 9 illustrates the profiles of inter-storey drift ratios of the two structures, i.e. the primary building (U) and the coupled system (C).

Table 3. Peak floor displacements (Ux, Uy) and inter-storey drift ratios (Δx, Δy) in x- and y-directions for the primary structure and the coupled system, DLS.

| | Primary structure | | | | Coupled system | | | |
|---|---|---|---|---|---|---|---|---|
| Level | $U_x$ [m] | $U_y$ [m] | $\Delta_x$ [‰] | $\Delta_y$ [‰] | $U_x$ [m] | $U_y$ [m] | $\Delta_x$ [‰] | $\Delta_y$ [‰] |
| 1 | 0.003 | 0.003 | 0.7 | 0.6 | 0.002 | 0.003 | 0.5 | 0.6 |
| 2 | 0.006 | 0.006 | 0.9 | 0.9 | 0.004 | 0.006 | 0.6 | 0.8 |
| 3 | 0.010 | 0.009 | 0.9 | 0.9 | 0.006 | 0.008 | 0.5 | 0.7 |
| 4 | 0.013 | 0.012 | 0.9 | 0.9 | 0.007 | 0.010 | 0.5 | 0.7 |
| 5 | 0.015 | 0.015 | 0.9 | 0.9 | 0.009 | 0.013 | 0.4 | 0.6 |
| 6 | 0.018 | 0.018 | 0.8 | 0.9 | 0.010 | 0.015 | 0.4 | 0.6 |
| 7 | 0.021 | 0.020 | 0.7 | 0.8 | 0.011 | 0.017 | 0.3 | 0.6 |
| 8 | 0.022 | 0.022 | 0.5 | 0.6 | 0.012 | 0.019 | 0.3 | 0.6 |
| 9 | 0.023 | 0.024 | 0.4 | 0.4 | 0.013 | 0.020 | 0.2 | 0.5 |

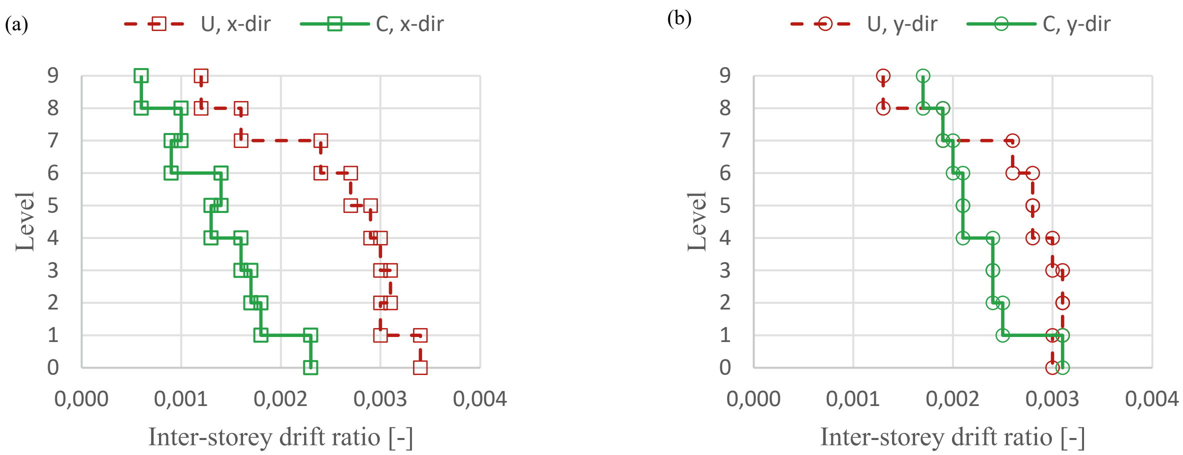


Fig. 9. Inter-storey drift ratios for the primary structure and the coupled system, DLS: (a) x-direction; (b) y-direction.

Outcomes are fully lower than the limit established by the Standards, so verifications have been proved. Correspondent numerical values ($\Delta_x, \Delta_y$ [‰]) can be found in the table at which the two diagrams of inter-storey drift ratios have been drawn (Table 3). Due to a similarity in displacements for the two buildings along y-direction, their inter-storey drift ratios become close at a same level almost coming to overlap themselves at the upper floors.

Dealing now with Life-safety Limit State, data concerning displacements are shown below:

Table 4. Peak floor displacements (Ux, Uy) in x- and y-directions for the primary structure and the coupled system, LLS.

| Level | Primary structure $U_x$ [m] | Primary structure $U_y$ [m] | Coupled system $U_x$ [m] | Coupled system $U_y$ [m] |
|---|---|---|---|---|
| 1 | 0.009 | 0.008 | 0.006 | 0.008 |
| 2 | 0.016 | 0.016 | 0.010 | 0.014 |
| 3 | 0.024 | 0.024 | 0.015 | 0.020 |
| 4 | 0.032 | 0.032 | 0.019 | 0.026 |
| 5 | 0.039 | 0.040 | 0.022 | 0.032 |
| 6 | 0.046 | 0.047 | 0.026 | 0.037 |
| 7 | 0.052 | 0.054 | 0.028 | 0.042 |
| 8 | 0.057 | 0.059 | 0.031 | 0.047 |
| 9 | 0.060 | 0.063 | 0.032 | 0.051 |

Floor displacements are clearly higher than those of DLS but they never still overcome a few centimetres. Along x-direction, the retrofitted construction achieves a huge reduction at the top passing from 6.00 to 3.20 cm, thus it is equal to -46.30%; in y-direction, positive effects of the external solution exist even if they are less significant. Concerning trends are illustrated in Figure 10:

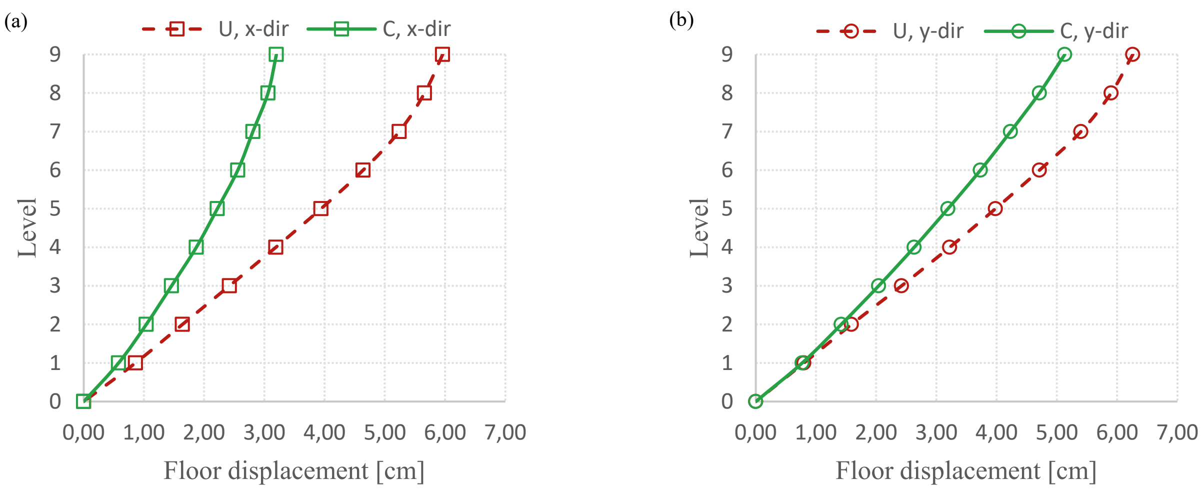


Fig. 10. Profiles of floor displacements for the primary structure and the coupled system, LLS: (a) x-direction; (b) y-direction.

Another subject to be addressed concerns base shears ($V_b$) whose results for both structures along each direction for Life-safety LS are reported in Table 5.

Table 5. Base shear forces ($V_b$) for the existing structure and the controlled system in x- and y-direction, LLS.

| $V_b$ [$kN$] | Primary structure | Coupled system |
|---|---|---|
| x-dir | 1575.03 | 3460.30 |
| y-dir | 1515.42 | 2371.18 |

The lowest floor of the Coupled system undergoes the greatest shear forces whose values are indicated in the abovementioned table; it happens because of the rise in mass, frequency and stiffness. Nevertheless, the connections allow the exoskeleton to bear the additional forces reducing those that act just on the primary structure and protecting it.

The effectiveness of the proposed method is also visible at the top level, where centre of gravity and centre of stiffness of the retrofitted system remain extremely close:

Table 6. Centres of gravity (G) and stiffness (K) of the Coupled system.

| | x [m] | y [m] |
|---|---|---|
| G (x,y) | 13.51 | 6.55 |
| K (x,y) | 13.50 | 6.55 |

Finally, the last analysis only concerns the steel that stands from the 1st to the 9th level in order to find the cost of the intervention per square meter (in other words, foundations and rigid links have not been considered). Estimating a steel price equal to $4\ €/kg$ that includes materials and installation, total cost can be derived. Then, gross area for each floor has been taken into account and multiplying it for the number of the levels, the entire gross surface is obtained. Finally, total cost is divided by the overall square meters and it now appears easy to understand if the solution turns out to be cost-effective: actually, it is. In fact, $185.08\ €/m^2$ is definitely less than the estimated cost for a traditional adjustment of an existing building that can be evaluated at almost $800\ €/m^2$. All the values can be found in the following table:

Table 7. Cost of the structural intervention.

| Total mass [kg] | Steel price [€/kg] | Total price [€] | Gross area/floor [m²] | Floor no. [-] | Gross area [m²] | *Adjustment price* [€/m²] |
|---|---|---|---|---|---|---|
| 185,521 | 4.00 | 742,084 | 445.50 | 9 | 4009.50 | 185.08 |

## 4. Conclusions

This study has been thought to find out if an external self-supporting steel structure could be an efficient solution to the seismic adjustment of a real reinforced concrete building and what kind of response it could present.
The research allowed to generate a dynamic system whose structural design could be adapted to the specific needs of the primary structure it is rigidly linked to. Subsequently, seismic analyses have been performed and concerning outcomes between the original structure and the retrofitted system are as follows:

- a floor displacements reduction for both Limit States;
- a growth of frequencies because of an increase in mass and stiffness;
- a more efficient behaviour occurs along x-direction given that it is stiffer than the transverse one;
- cost of operations is incredible lower than the price required for a traditional adjustment;
- preservation of the existing building that avoids both demolition and heavy reconstruction works, thanks to external operations;
- the overall sizes of this solution are nearly limited to the perimeter of the inner construction given that it just needs 1.50 m to incorporate the balconies and put the exoskeleton foundations beyond the existing ones; thus, it represents a useful answer to isolated urban structures that are no longer in compliance with the current technical standards.

As a result, the exoskeleton structure can cope with the problem of seismic adjustment of existing constructions even allowing them to achieve more performing energetic and aesthetic features.

## References

European Commission, 2012. "Energy-efficient buildings PPP beyond 2013-Research and Renovation Roadmap". Document for E2B European Initiative (ECTP).

Martelli L., Restuccia L., Ferro G.A., 2019. The exoskeleton: a solution for seismic retrofitting of existing buildings. Structural Integrity Procedia,1st Virtual Conference on Structural Integrity-VCSI1

ISTAT, Building census, < http://dati-censimentopopolazione.istat.it/Index.aspx?DataSetCode=DICA_EDIFICI1 >, 2011.

Belleri A., Marini A., 2016. Does seismic risk affect the environmental impact of existing buildings? Energy Build, 2016; 110:149–58.

Caverzan A., Lamperti Tornaghi M., Negro P., 2016. Proceedings of SAFESUST workshop - a roadmap for the improvement of earthquake resistance and eco-efficiency of existing buildings and cities, Publications Office of the European Union. https://doi.org/10.2788/499080.
Marini A., Passoni C., Riva P., Negro P., Romano E., Taucer F., 2014. Technology options for earthquake resistant, eco-efficient buildings in Europe: research needs. EUR 26497 EN JRC87425, Technical Report, Publications Office of the European Union. https://doi.org/10.2788/68902.
Reggio A., Restuccia L., Martelli L., Ferro G.A., 2019. Seismic performance of exoskeleton structures. Engineering Structures. https://doi. org/ 10.1016/j.engstruct.2019.109459
Martelli L., 2018. L'esoscheletro come approccio metodologico per l'adeguamento sismico di costruzioni esistenti. (Supervisor: Prof. G.A. Ferro). Master Degree Thesis, Politecnico di Torino.
Ministero delle Infrastrutture e dei Trasporti, 2018. Norme Tecniche per le Costruzioni, D.M. 18.01.2018, Rome.
Robot Structural Analysis Professional, Autodesk, <www.autodesk.com>, 2020.
Interdepartmental Ordinance no.1444, 1968. Art. 9, D.M. 1444/1968, Rome.
CSLP < http://cslp.mit.gov.it >, 2019.